Journal of Fractional Calculus and Nonlinear Systems

ifcns.sabapub.com ISSN: 2709-9547

J Frac Calc & Nonlinear Sys (2023)4(2):14-30

doi:10.48185/jfcns.v4i2.862

Haar wavelet approach to study the control of biological pest model in Tea plants

KUMBINARASAIAH S. a,* D, YESHWANTH R. a

^a Department of Mathematics, Bangalore University, Bengaluru-560056

• Received: 11 October 2023

• Accepted: 23 November 2023

• Published Online:27 December 2023

Abstract

In this study, we consider a novel approach called the Haar wavelet collocation method (HWCM) to examine the mathematical model of pest propagation in tea plants and how biological enemies might control them. This model is in the form of a system of coupled ordinary differential equations (ODEs). When studying the system, we consider tea plants, pests that harm the plants, biological enemies that are their reasonable competitors of pests, self-reproduction of the tea plants, natural death of pests and natural enemies, etc. By turning the Mathematical model into a system of non-linear algebraic equations, we use the properties of the Haar wavelets. The opted method can solve the biological pest management problem in tea plants. The values of the unknown coefficients are recovered using the collocation method and Newton Raphson method. The Mathematica program acquires the numerical results, nature, and uniformity. The acquired findings show that the current method is more accurate than those indicated in tables and graphs.

Keywords: Haar wavelet method, Collocation method, Non-linear Ordinary differential equations. 2010 MSC: 65T60, 97M60, 35A24.

1. Introduction

Tea is regarded as a beverage and a gift from nature to humans for starting a new day, making it the second most popular beverage in the world after water. Asia is home to most tea-producing nations, with China, India, and Sri Lanka being the three biggest producers [1]. Black, yellow, green, and white tea originates from the same Camellia sinensis plant. India produces 52% of the world's tea, with the State of Assam being the primary producer. Under various agroecological conditions, tea is grown in the tropics and subtropics in different porous, well-drained, acidic soil types (PH 3.3 to 6.0). It is subjected to various climatic conditions, including temperatures between 12°C and 40°C, annual rainfall between 938 and 6000 mm, and relative humidity ranging from 30 percent to 90 percent. Tea trees can reach a height of 15 m in the wild [2, 3]. Since tea plants can live for anywhere between 30 and 50 years, [2] fighting off diseases and pests is

^{*}Corresponding author: kumbinarasaiah@gmail.com

one of the important jobs for tea growers (Figure 1). Pests will quickly impact the tea plants because this is the time of year when tea growers can harvest their produce from mid-March to mid-November.

Therefore, pests become unavoidable visitors in every cropping system and lower plant growth, harm various plant sections, and lower crop quality and productivity. The insects use their mouth styles to suck sap from buds, terminal twigs, and leaves while injecting them with their deadly saliva [4]. As a result, the once-fresh and healthy leaves slowly distort and curl up. An unfavorable environment causes the plant to die from the tips of its leaves or roots backward. Every female insect looks for soft plant tissues to lay 500–600 eggs. The eggs hatch after a week, and the nymphs are released. It takes approximately a month for a life cycle to complete. Pests can also come in different generations. After monsoon rainfall, damp and shaded regions experience the greatest pest impact. Agrotechnology is used to boost productivity while simultaneously increasing the number of losses as tea plant yield rises. One insect can cause numerous crop loss estimates. Its production affects various nations' national economies in different ways. Insect and mite pests (arthropods) are often responsible for 5% to 55% of the damage [5, 6, 7, 8]. Pests can be controlled using a variety of techniques. They mainly consist of applied control methods and natural control variables. Climate variables, topography features, predators and parasites, and other things are examples of natural controls. The following applied control methods are also used: physical control, cultural control, microbial control, biological control, mechanical control, regulatory control, chaemosterilant, breeding resistant agrotypes, chemical control, ionizing radiation, and so on [9].

Nature uses a variety of strategies to defend plants from pest species, with biological control being one of the most effective and environmentally friendly [8, 10]. In contrast to chemical pesticides, natural enemies are used in biological control approaches to suppress pest species (see Figure 2). The use of natural enemies to control pests is referred to as "biological control" in this context. The only strategy that is both ecologically friendly and increases species diversity while preserving biodiversity is biological control within an agroecosystem. By attacking the insects, viruses, bacteria, and fungi that harm the plants, a natural enemy maintains the ecosystem's equilibrium and reduces the population of pests [10]. Predators, diseases, or parasitoids are just a few examples of the natural enemies of pests. When compared to chemical control, biological control approaches have several advantages. They are:

- 1. Natural enemies help to reduce pest populations permanently;
- 2. The likelihood of bug resistance growth diminishes when biological control techniques are used. All types of pests, including potentially hazardous and beneficial species, are eliminated by pesticides. Using natural enemies to control pests is a successful and efficient method since they exclusively attack and kill their intended targets, making them ideal for eradicating certain pests.

The successful and practical result of in-depth research has been the widespread and extended application of biological control. It entails examining and identifying regional natural enemies (such as diseases, parasitoids, and predators) in tea ecosystems, raising awareness of their ecological and biological importance, and creating methods for breeding and releasing natural enemies in tea plantations. Ordinary differential equations have



Figure 1: Biological enemies for the Tea plant.

contributed significantly to the history of ecology and will continue to do so in the years to come. Many scholars have used three-species food chain models to comprehend the dynamics of multispecies interaction in the ecology [12, 13, 14]. [14] presents the stability dynamics of a three-species model with a complicated character. You may see some of the research using three-species models to represent the dynamics of pests in [7, 10]. In this article, we considered the model proposed in [11], which describes three communities: the tea plants (x), the pests that harm them (y), such as whiteflies and small moth larvae, etc., and their biological adversaries (such as predatory chrysopids, carabids, and Agelena labyrinthica), which are also their justifiable competitors (z). It is believed that timely harvesting of tea plants can stop insect damage.

$$\begin{cases} \frac{dx}{dt} = r_1 x - c_1 x^2 - \frac{\delta_1 x y}{q_0 + x + s_0 y} - h x, \\ \frac{dy}{dt} = \frac{\delta_2 x y}{q_0 + x + s_0 y} - \frac{\delta_3 y z}{q_1 + y + s_1 z} - \mu_1 y, \\ \frac{dz}{dt} = \frac{\delta_4 y z}{q_1 + y + s_1 z} - \mu_2 z, \end{cases}$$
(1.1)

with assumed initial conditions,

$$x(0) = x_0, y(0) = y_0, z(0) = z_0.$$

where, r_1 , c_1 , h, δ_1 , δ_2 , δ_3 , δ_4 , μ_1 , μ_2 , q_0 , q_1 , s_0 , s_1 are all non-negative parameters. Here, r_1 represents the rate at which tea plants reproduce on their own, c_1 represents the level of competition among tea plants for resources like food and space, μ_1 represents the natural mortality rate of the pest population in the absence of tea plants, and μ_2 represents the natural mortality rate of natural enemies in the absence of pests. The parameters δ_1 and δ_3 show, respectively, the per capita rate of pest predation on tea plants and that of natural enemies on pests, whereas δ_2 and δ_4 show, respectively, the effectiveness of biomass conversion from tea plants to pests and from pests to natural enemies. The parameters q_0 and q_1 represent the environmental protection offered to tea plants and pests, respectively, s_0 represents the level of pest-pest interaction, s_1 represents the level of natural enemy interaction, and h represents the harvesting effort. The rate of self-reproduction of tea plants is thought to be higher than the pace of harvesting.

Wavelet theory is a recent promising area in mathematical research. It has been used in various domains, including signal analysis for representing and segmenting waveforms,

time-frequency analysis, biological field, and quick methods for straightforward implementation. In the middle of the 1980s, wavelet theory emerged, having a major impact on both pure and practical mathematics. Due to their properties, such as orthogonality, compact support, and ability to provide a precise representation of a variety of functions and operators at different levels of resolution, wavelet methods have attracted a lot of attention in the last three decades for the numerical solution of differential equations [15, 16]. There are different wavelet methods, for instance, the Haar wavelet method on ODEs [17, 18], Haar wavelets matrix through linear algebra [19], Haar wavelet collocation technique for fractal-fractional order problem [31], Haar wavelet method for the study of two-phase nanofluid MHD boundary layer flow [20], Laplace transform method for Thermo-diffusion effect on magnetohydrodynamics flow of fractional Casson fluid [29], Enhancement of heat and mass transfer of a physical model using Laplace transform method [30], Haar wavelet method for Fractional Fredholm Integro-differential equations [21], Haar wavelet method for Third order Integro Differential Equations [33], Numerical solution of higher order nonlinear integro differential equations involving variable coefficients using Haar wavelets [34], Solution of Mittag-Leffler type Fractional Fredholm Integro-differential equations using Haar wavelet techniques [32], Numerical solution for the HIV infection of CD4+ Tcells model using Modified Bernoulli wavelets [22], Solution of a system of differential equations using Laguerre wavelets [23], Taylor wavelet approach for the linear and nonlinear singular value problems [24], Hermite wavelet technique to solve mathematical models on the digestive system and COVID-19 pandemic [25]. In this article, the Haar wavelet method was developed to resolve differential equations, demonstrating its effectiveness and strength. The obtained results are compared with the ND Solver solution. The proposed approach provides the easiest and most effective way of solving the proposed model. In the literature survey, no one considered this model by HWCM; this motivates us to study this model by the present method. The arrangements for the rest of the paper are the fundamentals of the Haar wavelet concept and attributes described in section 2, which outlines the structure for the remaining study. In section 3, certain theorems on the Haar wavelet are presented. Section 4 offers

2. Preliminaries of the Haar Wavelets

conclusions are drawn in section 6.

Consider an interval $[a,b]\subset\mathbb{R}$ which is divided into 2M subintervals of equal length; the length of each subinterval is $\Delta x=(b-a)/2M$. Now two parameters are introduced: j=0,1,2,...,J and k=0,1,2,...,m-1, where $m=2^j$. The wavelet number i is identified as i=m+k+1. where j is called the dilation parameter, and k is called the translation parameter. Then the i^{th} Haar wavelet is, then described as

the procedure for solving differential equations. Numerical results are shown in 5. Finally,

$$h_{\mathbf{i}}(x) = \begin{cases} 1 & \text{for } x \in [\zeta_1(\mathbf{i}), \zeta_2(\mathbf{i})), \\ -1 & \text{for } x \in [\zeta_2(\mathbf{i}), \zeta_3(\mathbf{i})), \\ 0 & \text{otherwise} \end{cases}$$
 (2.1)

where,

$$\zeta_1(i) = \alpha + 2k\lambda \Delta x, \tag{2.2}$$

$$\zeta_2(i) = \alpha + (2k+1)\lambda \Delta x, \tag{2.3}$$

$$\zeta_3(i) = \alpha + 2(k+1)\lambda \Delta x, \tag{2.4}$$

$$\lambda = \frac{M}{m}. (2.5)$$

(2.1) is valid for i > 2. For i=1 we have,

$$h_1(x) = \begin{cases} 1 & \text{for } x \in [a, b), \\ 0 & \text{otherwise.} \end{cases}$$
 (2.6)

(2.6) called the Haar scalar function. The operational matrix of integration are given by,

$$p_{\beta,i}(x) = \int_{a}^{x} \int_{a}^{x} \int_{a}^{x} ... \int_{a}^{x} h_{i}(x) dx^{\beta},$$
 (2.7)

where, i = 1, 2, ..., 2M, $\beta = 1, 2, ..., n$, and for i=1, we have

$$p_{\beta,1}(x) = \frac{1}{\beta!}(x-\alpha)^{\beta},$$
 (2.8)

for $i \ge 2$, we have

$$p_{\beta,i}(x) = \begin{cases} 0 & \text{for} \quad x < \zeta_1(i) \\ \frac{1}{\beta!}[x - \zeta_1(i)]^\beta & \text{for} \quad x \in [\zeta_1(i), \zeta_2(i)], \\ \frac{1}{\beta!}\{[x - \zeta_1(i)]^\beta - 2[x - \zeta_2(i)]^\beta\} & \text{for} \quad x \in [\zeta_2(i), \zeta_3(i)], \\ \frac{1}{\beta!}\{[x - \zeta_1(i)]^\beta - 2[x - \zeta_2(i)]^\beta + [x - \zeta_3(i)]^\beta\} & \text{for} \quad x > \zeta_3(i). \end{cases}$$

For the particular value of J=2 the first order operational matrix of integration is represented as

$$p_1(x) = \begin{bmatrix} 0.0625 & 0.1875 & 0.3125 & 0.4375 & 0.5625 & 0.6875 & 0.8125 & 0.9375 \\ 0.0625 & 0.1875 & 0.3125 & 0.4375 & 0.4375 & 0.3125 & 0.1875 & 0.0625 \\ 0.0625 & 0.1875 & 0.1875 & 0.0625 & 0 & 0 & 0 & 0 \\ 0 & 0 & 0 & 0 & 0.0625 & 0.1875 & 0.1875 & 0.0625 \\ 0.0625 & 0.0625 & 0 & 0 & 0 & 0 & 0 & 0 \\ 0 & 0 & 0.0625 & 0.0625 & 0 & 0 & 0 & 0 \\ 0 & 0 & 0 & 0 & 0.0625 & 0.0625 & 0 & 0 \\ 0 & 0 & 0 & 0 & 0 & 0.0625 & 0.0625 & 0 & 0 \\ 0 & 0 & 0 & 0 & 0 & 0 & 0.0625 & 0.0625 \end{bmatrix}$$

3. Some results on the Haar wavelets

For every pair of i, $j \in \mathbb{Z}$, the Haar function $\psi_{i,j}$ is defined on \mathbb{R} as, $\psi_{i,j}(x) = 2^{\frac{i}{2}} \psi(2^i x - j)$, $\forall x \in \mathbb{R}$. This function is supported on $\left[\frac{j}{2^i}, \frac{(j+1)}{2^i}\right)$ with the property $\int_{\mathbb{R}} \psi_{i,j}(x) dx = 0$ and $||\psi_{i,j}||_2^2 = \int_{\mathbb{R}} \psi_{i,j}^2(x) dx = 1$.

Theorem 3.1. Let $\{\psi_{i,j}(x)|i,j\in\mathbb{Z}\}$ be set of the Haar system functions on \mathbb{R} . Then $L^2(\mathbb{R})$ be the Haar space is complete.

Proof. Let $\{\psi_{i,j}(x)|i,j\in\mathbb{Z}\}$ be the basis of the normed linear space $L^2(\mathbb{R})$. Consider $\{\psi_{i,j}^k\}$ be the Haar cauchy sequence in $L^2(\mathbb{R})$. By the definition of cauchy sequence for a given $\varepsilon=\frac{1}{2}>0,\ \exists\ a$ +ve integer $\eta_1\ni$: $\|\psi_{i,i}^{k} - \psi_{i,i}^{l}\|_{2} < \frac{1}{2}, \ \forall k, l \geqslant \eta_{1}$

for $\epsilon = \frac{1}{2}$, choose $\psi_{i,j}^{k_1}$, such that $\|\psi_{i,j}^{k_1} - \psi_{i,j}^{k_2}\|_2 < \frac{1}{2}$, $\forall k_1, k_2 \geqslant \eta_1$ for $\epsilon = \frac{1}{2^2}$, choose $\psi_{i,j}^{k_2}$, such that $\|\psi_{i,j}^{k_2} - \psi_{i,j}^{k_3}\|_2 < \frac{1}{2^2}$, $\forall k_2, k_3 \geqslant \eta_2$

for $\varepsilon=\frac{1}{2^n}$, choose $\psi_{i,j}^{k_n}$ such that $\|\psi_{i,j}^{k_n}-\psi_{i,j}^{k_{n+1}}\|_2<\frac{1}{2^n},\ \forall k_n,k_{n+1}\geqslant \eta_n$ $\begin{array}{l} \dots\{\psi_{i,j}^{k_n}\} \text{ is subsequence of }\{\psi_{i,j}^k\}. \text{ It is clear that, } \sum\limits_{k=1}^{\infty}\|\psi_{i,j}^{k_{n+1}}-\psi_{i,j}^{k_n}\|_2\leqslant \sum\limits_{n=1}^{\infty}\frac{1}{2^n}=1. \\ \text{Consider, } \varphi_n=|\psi_{k_1}|+|\psi_{k_2}-\psi_{k_1}|+,\cdots,+|\psi_{k_{n+1}}-\psi_{k_n}|, \text{ for } n=1,2,3,\cdots \\ \Longrightarrow\{\varphi_n\} \text{ is an increasing sequence of non-negative measurable functions, such that } \\ \end{array}$ $\| \varphi_n \|_2^2 = [\| \psi_{k_1} \|_2 + \sum_1 \| \psi_{k_{n+1}} - \psi_{k_n} \|_2]^2 \, \check{\ } \, ,$ (by Minkowski inequality)

 $\|\varphi_n\|_2^2\leqslant (\|\psi_{k_1}\|_2+1)^2<\infty.$ Therefore φ_n is bounded and increasing sequence, then \exists φ such that $\lim_{n\to\infty}\varphi_n=\varphi$, by monotone converging the sequence φ_n is bounded and increasing sequence. gence theorem, we have $\int \varphi^2 dx = \lim_{n \to \infty} \int \varphi_n^2 dx < \infty \implies \varphi \in L_p(\mathbb{R}).$

 $\implies \text{ The series } \psi_{k_1}(x) + \sum_{l}^{\infty} |\psi_{k_{n+1}}(x) - \psi_{k_n}(x)| \text{ converges almost eveywhere.}$ so that $\{\psi_{k_n}\}$ converges to $\psi(x)$, $\forall x \in A$, where A is measurable set. Further, let $\varepsilon > 0$ be given choose l so large such that $||\psi_{i,j}^k - \psi_{i,j}^l||_2 < \varepsilon$, $\forall k, l \geqslant L$

$$\implies \|\psi_{i,j}^k - \psi_{i,j}^{l_n}\|_2 < \epsilon, \qquad \forall k, l_n \geqslant L$$

$$\implies \left[\int |\psi_{i,j}^k - \psi_{i,j}^{l_n}|^2 dx\right] < \epsilon^2$$
 (by Fatou's Lemma)

$$\int |\psi - \psi_{i,j}^{k}|^2 dx = \int \lim_{k \to \infty} |\psi_{i,j}^{n_k} - \psi_{i,j}^{k}|^2 dx < \epsilon^2 < \infty$$

$$\begin{aligned} & \Longrightarrow \|\psi_{i,j}^{k} - \psi_{i,j}^{l_n}\|_2 < \varepsilon, \qquad \forall k, l_n \geqslant L \\ & \Longrightarrow \|\psi_{i,j}^{k} - \psi_{i,j}^{l_n}\|_2 < \varepsilon, \qquad \forall k, l_n \geqslant L \\ & \Longrightarrow [\int |\psi_{i,j}^{k} - \psi_{i,j}^{l_n}|^2 dx] < \varepsilon^2 \qquad \text{(by Fatou's Lemma),} \\ & \int |\psi - \psi_{i,j}^{k}|^2 dx = \int \lim_{k \to \infty} |\psi_{i,j}^{n_k} - \psi_{i,j}^{k}|^2 dx < \varepsilon^2 < \infty, \\ & \text{Thus, } \psi - \psi_{i,j}^{k} \in L_p(\mathbb{R}) \text{ and } \psi = \psi - \psi_{i,j}^{k} + \psi_{i,j}^{k} \in L_p(\mathbb{R}) \text{ and } \lim_{n \to \infty} \|\psi - \psi_{i,j}^{k}\|_2 = 0. \end{aligned}$$

Thus ψ is limit in $L_2(\mathbb{R})$ of sequence $\{\psi_{i,i}^k\}$. Hence $L_p(\mathbb{R})$ is complete.

Theorem 3.2. Let us assume that $f(x) = \frac{d^n u(x)}{dx^n} \in L^2(\mathbb{R})$ is a continuous function on [0,1] and its first derivative is bounded $\forall x \in [0,1], \, n \geqslant 2$. Then the Haar wavelet method, based on approach proposed in [27, 28], will be convergent. i.e. $|E_M|$ vanishes as J goes to infinity. The convergence is of order two [26] as following, $\|\mathbf{E}_{\mathbf{M}}\|_2 = O\left[\left(\frac{1}{2^{J+1}}\right)^2\right].$

Solution at collocation points: Let μ is set of all collocation points which is measurable. $\{C_i\}$ be the sequence of collocation points and $\{f_i\}$ be the sequence of functional values at $\{C_i\}$ that satisfies the given system of differential equations. Here f be a function from \mathbb{Z}^+ to \mathbb{R} defined by $f(\mathfrak{i})=f_\mathfrak{i}$. Then

$$f(x) = \sum_{i=1}^{\infty} f(i),$$

where f(x) is an exact solution of a given system of differential equations.

4. Method of Solution For Tea Model

Consider the system of n-differential equations as follows:

$$\begin{aligned} y_{1}^{'}(x) &= f_{1}(t, y_{1}(x), ..., y_{n}(x)), \\ y_{2}^{'}(x) &= f_{2}(t, y_{1}(x), ..., y_{n}(x)), \\ &\vdots \\ y_{n}^{'}(x) &= f_{n}(t, y_{1}(x), ..., y_{n}(x)), \end{aligned} \tag{4.1}$$

with initial conditions $y_k(0) = \alpha_k$, k = 1, 2, ..., n. In order to find the Haar wavelet solution of these system of differential equations. We first find the collocation points using collocation method.i.e, given by

$$x_1 = 0.5(\tilde{x_{1-1}} + \tilde{x_1}),$$
 $l = 1, 2, ..., 2M.$

Where,

$$\tilde{x_l} = a + l\Delta x,$$
 $l = 0, 1, 2, ..., 2M.$

Now the Haar wavelet approximation of (4.1) can be written as

$$y'_{k}(x) = \sum_{i=1}^{2M} a_{i}^{k} h_{i}(x).$$
 (4.2)

Integrating (4.2) with respect to x from 0 to x, we ge

$$y_k(x) = y_k(0) + \sum_{i=1}^{2M} a_i^k P_{i,i}(x).$$
 (4.3)

Where, $P_{1,i}$ is first operational matrix of integration. Substituting the equations (4.2) and (4.3) in (4.1) and replacing x by x1 the system of differential equations reduces to system of algebraic equations as follows:

$$\begin{split} F_{1}(a_{1}^{1},a_{2}^{1},...,a_{2M}^{1},a_{1}^{2},a_{2}^{2},...,a_{2M}^{2},...,a_{1}^{n},a_{2}^{n},...,a_{2M}^{n}) &= 0 \\ F_{2}(a_{1}^{1},a_{2}^{1},...,a_{2M}^{1},a_{1}^{2},a_{2}^{2},...,a_{2M}^{2},...,a_{1}^{n},a_{2}^{n},...,a_{2M}^{n}) &= 0 \\ & \vdots \\ F_{n}(a_{1}^{1},a_{2}^{1},...,a_{2M}^{1},a_{1}^{2},a_{2}^{2},...,a_{2M}^{2},...,a_{1}^{n},a_{2}^{n},...,a_{2M}^{n}) &= 0. \end{split}$$

$$(4.4)$$

To find the values of Haar coefficients a_i^k , we considered the Newton-Raphson method as follows: If the initial guess of the root is a_i^k and a_{i+1}^k is the point at which the slope intercepts, then the Taylor series expansion of (4.4) can be written as

$$F_{1,i+1} = F_{1,i} + (a_{1,i+1}^k - a_{1,i}^k) \frac{\partial F_{1,i}}{\partial a_1^k} + (a_{2,i+1}^k - a_{2,i}^k) \frac{\partial F_{1,i}}{\partial a_2^k} + \dots + (a_{2M,i+1}^k - a_{2M,i}^k) \frac{\partial F_{1,i}}{\partial a_{2M}^k}, \tag{4.5}$$

where, k=1,2,3,...,n. Applying the Taylor expansion similarly for $F_2, F_3, F_4, ..., F_n$. And generalizing for n equations, we get

$$\frac{\partial F_{k,i}}{\partial \alpha_1^k} \alpha_{1,i+1}^k + \frac{\partial F_{k,i}}{\partial \alpha_2^k} \alpha_{2,i+1}^k + ,..., \\ + \frac{\partial F_{k,i}}{\partial \alpha_{2M}^k} \alpha_{2M,i+1}^k = -F_{k,i} + \alpha_{1,i}^k \frac{\partial F_{k,i}}{\partial \alpha_1^k} + \alpha_{2,i}^k \frac{\partial F_{k,i}}{\partial \alpha_2^k} + ,..., \\ + \alpha_{2M,i}^k \frac{\partial F_{k,i}}{\partial \alpha_{2M}^k}, \quad (4.6)$$

the first subscript k represents the equations in (4.4), and the second subscript denotes the function value at the present value (i) or at the next value (i+1). (4.6) can be represented in matrix notation as:

$$[J][a_{i+1}^k] = -[F] + [J][a_i^k]. \tag{4.7}$$

where the partial derivatives evaluated at i are written as the Jacobian matrix consisting of partial derivatives:

$$[J] = \begin{bmatrix} \frac{\partial F_{1,i}}{\partial \alpha_1^k} & \frac{\partial F_{1,i}}{\partial \alpha_2^k} & \cdots & \frac{\partial F_{1,i}}{\partial \alpha_{2M}^k} \\ \frac{\partial F_{2,i}}{\partial \alpha_1^k} & \frac{\partial F_{2,i}}{\partial \alpha_2^k} & \cdots & \frac{\partial F_{2,i}}{\partial \alpha_{2M}^k} \\ \vdots & & & \vdots \\ \frac{\partial F_{n,i}}{\partial \alpha_1^k} & \frac{\partial F_{n,i}}{\partial \alpha_2^k} & \cdots & \frac{\partial F_{n,i}}{\partial \alpha_{2M}^k} \end{bmatrix}$$

The initial and final values are expressed in vector form as:
$$[\alpha_i^k]^T = \begin{bmatrix} \alpha_{1,i}^k & \alpha_{2,i}^k & \cdots & \alpha_{2M,i}^k \end{bmatrix}, \ [\alpha_{i+1}^k]^T = \begin{bmatrix} \alpha_{1,i+1}^k & \alpha_{2,i+1}^k & \cdots & \alpha_{n,i+1}^k \end{bmatrix}, \ \text{and} \quad [F]^T = \begin{bmatrix} F_{1,i} & F_{2,i} & \cdots & F_{n,i} \end{bmatrix}.$$

Multiplying the inverse of the Jacobian to (4.7)

$$[a_{i+1}^k] = [a_i^k] - [J]^{-1}[F]. \tag{4.8}$$

from (4.8) we get the Haar wavelet Co efficients $a_i^k s$. Using $a_i^k s$ in Eqn (4.3) we get the desired solution of the Tea model(4.1).

t	ND Solver	Absolute Error of HWCM	Absolute Error of HWCM	Absolute Error of HWCM
	solution	(J=6) with ND Solver solution	(J=8) with ND Solver solution	(J=10) with ND Solver solution
0.1	8.961314	1.1173×10^{-2}	6.6365×10^{-3}	4.1284×10^{-4}
0.2	4.313439	3.5351×10^{-2}	2.1042×10^{-3}	1.3074×10^{-4}
0.3	2.557495	1.7084×10^{-2}	1.017×10^{-3}	6.3148×10^{-5}
0.4	1.630257	9.7483×10^{-3}	5.8032×10^{-4}	3.5836×10^{-5}
0.5	1.072577	6.0138×10^{-3}	3.5816×10^{-4}	2.2175×10^{-5}
0.6	0.716553	3.8618×10^{-3}	2.3004×10^{-4}	1.4215×10^{-5}
0.7	0.482494	2.5346×10^{-3}	1.5101×10^{-4}	9.3110×10^{-6}
0.8	0.326284	1.6841×10^{-3}	1.0030×10^{-4}	6.1148×10^{-6}
0.9	0.221197	1.1271×10^{-3}	6.7163×10^{-5}	4.1054×10^{-6}
1.0	0.150194	7.5768×10^{-4}	4.5185×10^{-5}	2.7840×10^{-6}

Table 1: Numerical comparison ND Solver solution and AE of HWCM for x(t)

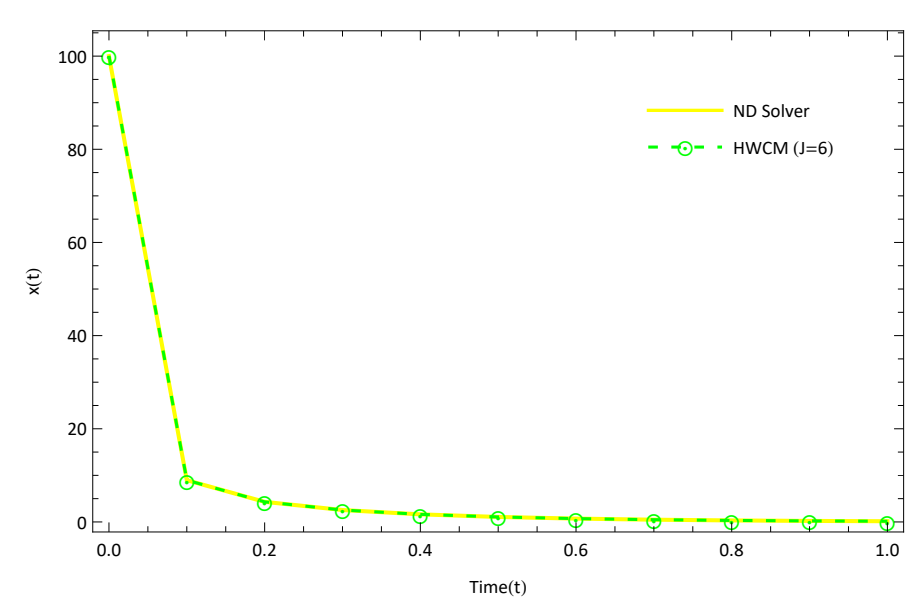


Figure 2: Graphical representation of HWCM (J=6), ND Solver solution for x(t)

5. Numerical Example and Discussion

The Tea model (1.1) is solved using the present approach called Haar wavelet collocation method(HWCM) with following initial conditions: x(0) = 100, y(0) = 10, z(0) = 5, and the parameter values $r_1 = 1$, $c_1 = 1$, $\delta_1 = 1.667$, $\delta_2 = 1.667$, $\delta_3 = 0.05$, $\delta_4 = 0.05$, $\mu_1 = 0.2443$, $\mu_2 = 0.01$, $q_0 = 0.334$, $q_1 = 0.6$, $s_0 = 0.334$, $s_1 = 0.5$, q = 0.25 and the obtained results are discussed in the Tables 1-3, and Figures 2-13. The numerical values of the HWCM are compared with the NDSolver solution and the Absolute Error is tabulated in Tables 1-3, Table 1 represent the numerical values of tea plants x(t), Table 2 represent the numerical values of pests that harm tea plants y(t) such as whiteflies, small moth larvae, etc., and Table 3 represent the numerical values of justifiable biological competitors z(t) for different values of J=6, 8, 10. We can see that error decreases with an increase in the resolution of HWCM. Graphical comparison of HWCM and NDSolver for x(t) Tea Plants, y(t) the pests that damage the tea plants, and z(t) also their justifiable biological competitors are shown in Figures 2-4 Figure 5 represents graphical representation of Absolute Error of HWCM(J=6,8,10) with ND Solver solution of tea plants x(t), Figure 6 represents graphical representation of Absolute Error of HWCM(J=6,8,10) with ND Solver solution of pests that harm tea plants y(t) such as whiteflies, small moth larvae, etc., Figure 7 represents graphical representation of Absolute Error of HWCM(J=6,8,10) with ND Solver solution of justifiable biological competitors z(t).

Effect of Self reproduction rate (r_1) : Figures 8-10 represent the changes of x(t), y(t), z(t) due to increase

	table 2. Numerical comparison ND bolver solution and NE of 11W GW for y(t)						
t	ND Solver	Absolute Error of HWCM	Absolute Error of HWCM	Absolute Error of HWCM			
	solution	(J=6) with ND Solver solution	(J=8) with ND Solver solution	(J=10) with ND Solver solution			
0.1	11.161210	4.0290×10^{-3}	2.3477×10^{-4}	1.4595×10^{-5}			
0.2	11.992991	8.8063×10^{-3}	5.1731×10^{-4}	3.2160×10^{-5}			
0.3	12.544911	1.2529×10^{-3}	7.3829×10^{-4}	4.5885×10^{-5}			
0.4	12.866949	1.5254×10^{-3}	9.0034×10^{-4}	5.5941×10^{-5}			
0.5	13.008189	1.7144×10^{-3}	1.0128×10^{-4}	6.2907×10^{-5}			
0.6	13.012975	1.8374×10^{-3}	1.0861×10^{-4}	6.7441×10^{-5}			
0.7	12.918519	1.9103×10^{-3}	1.1296×10^{-4}	7.0129×10^{-5}			
0.8	12.754298	1.9465×10^{-3}	1.1514×10^{-4}	7.1501×10^{-5}			
0.9	12.542666	1.9567×10^{-3}	1.1576×10^{-4}	7.1851×10^{-5}			
1.0	12.300027	1.9487×10^{-4}	1.1531×10^{-4}	7.1530×10^{-5}			

Table 2: Numerical comparison ND Solver solution and AE of HWCM for y(t)

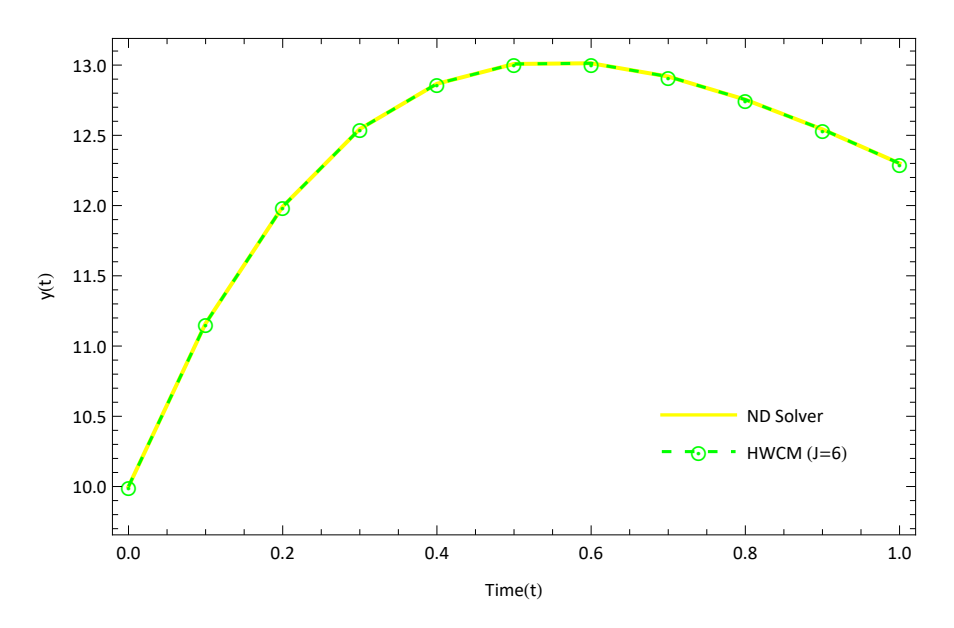


Figure 3: Graphical representation of HWCM (J=6), ND Solver solution for y(t)

Table 3: Numerical comparison ND Solver solution and AE of HWCM for z(t)

t	ND Solver	Absolute Error of HWCM	Absolute Error of HWCM	Absolute Error of HWCM
	solution	(J=6) with ND Solver solution	(J=8) with ND Solver solution	(J=10) with ND Solver solution
0.1	5.014359	2.5601×10^{-7}	1.3229×10^{-8}	8.1434×10^{-10}
0.2	5.029136	2.6631×10^{-6}	1.5446×10^{-7}	9.5960×10^{-9}
0.3	5.044185	6.2762×10^{-6}	3.6714×10^{-7}	2.2817×10^{-8}
0.4	5.059411	1.0723×10^{-5}	6.2930×10^{-7}	3.9094×10^{-8}
0.5	5.074743	1.5774×10^{-5}	9.2739×10^{-7}	5.7623×10^{-8}
0.6	5.090134	2.1285×10^{-5}	1.2527×10^{-7}	7.7824×10^{-8}
0.7	5.105546	2.7161×10^{-5}	1.5998×10^{-6}	9.9368×10^{-8}
0.8	5.120955	3.3339×10^{-5}	1.9648×10^{-6}	1.2199×10^{-7}
0.9	5.136339	3.9778×10^{-5}	2.3453×10^{-6}	1.4561×10^{-7}
1.0	5.151683	4.6447×10^{-5}	2.7394×10^{-6}	1.7008×10^{-7}

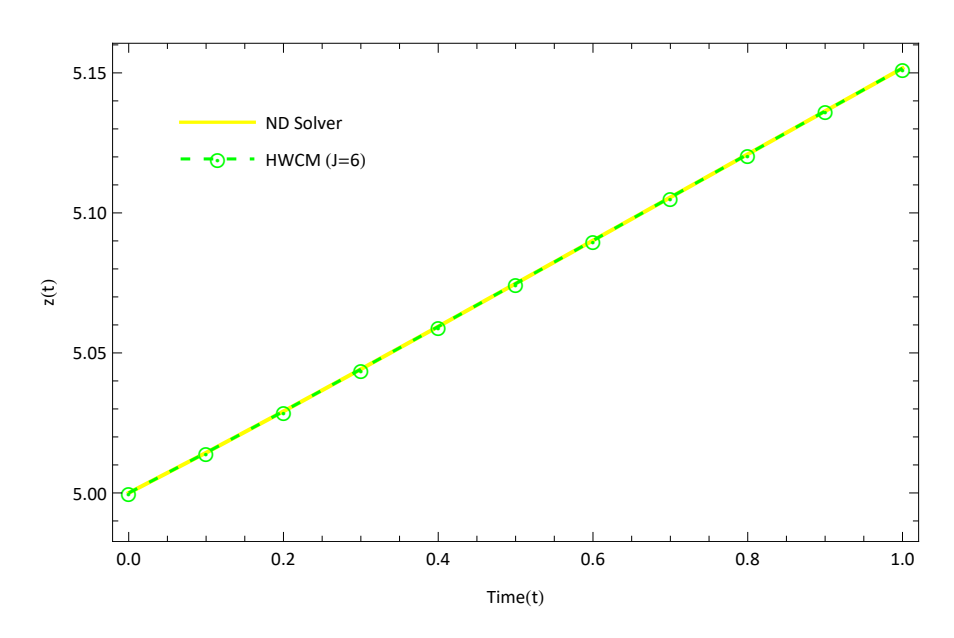


Figure 4: Graphical representation of HWCM (J=6),ND Solver solution for z(t)

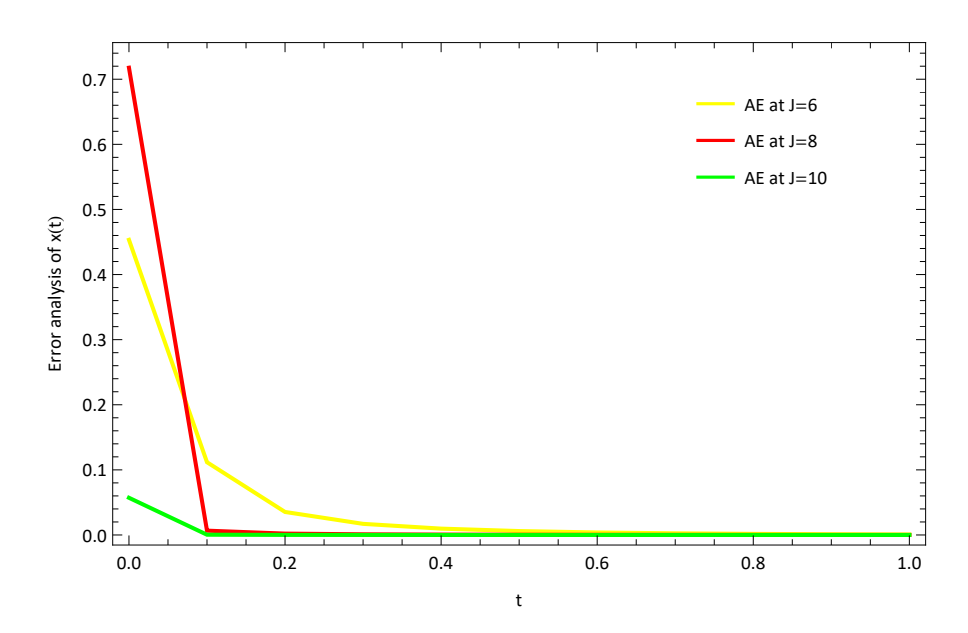


Figure 5: Graphical representation of Absolute Error of HWCM(J=6,8,10) with ND Solver solution for x(t)

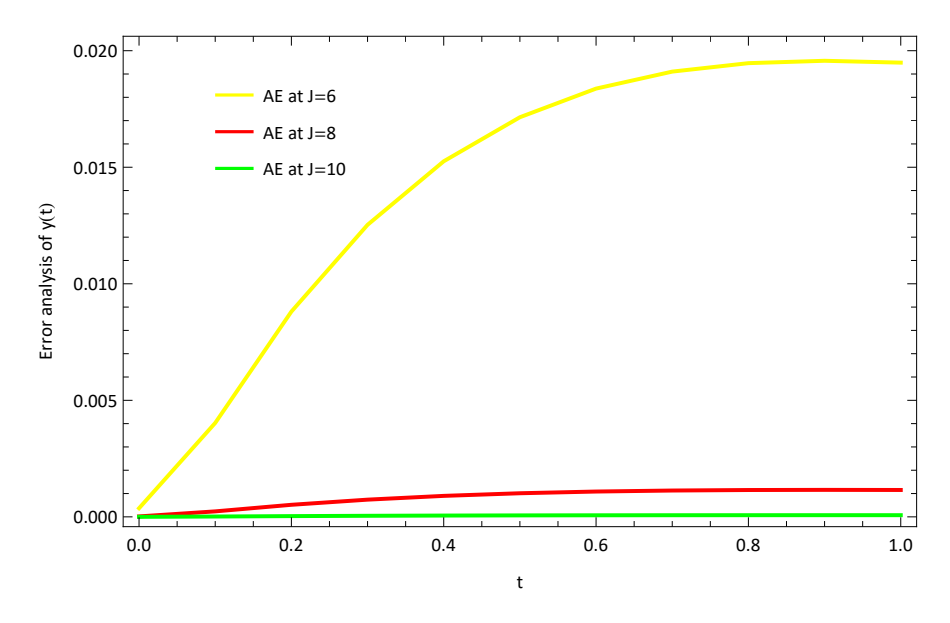


Figure 6: Graphical representation of Absolute Error of HWCM(J=6,8,10) with ND Solver solution for y(t)

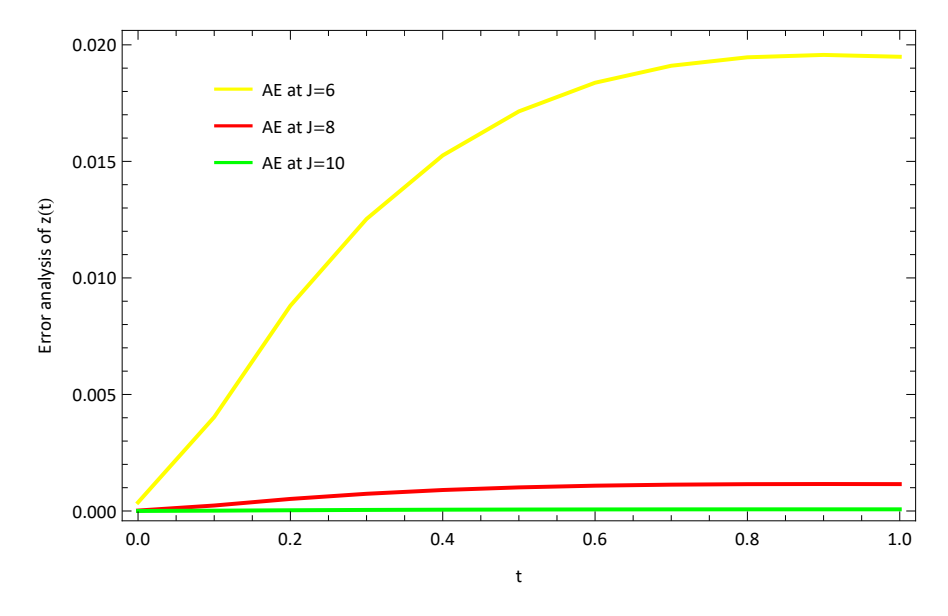


Figure 7: Graphical representation of Absolute Error of HWCM(J=6,8,10) with ND Solver solution for z(t)

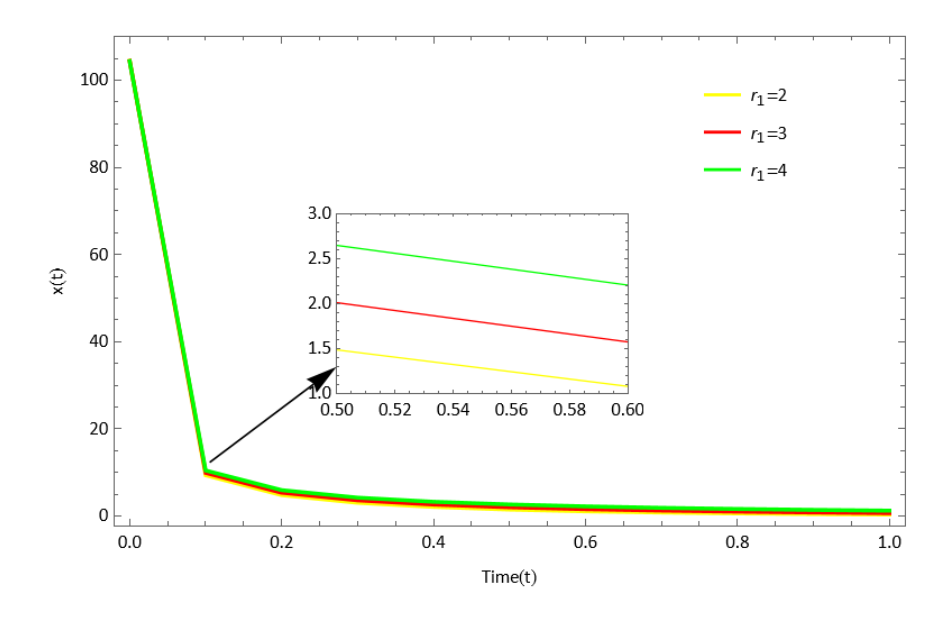


Figure 8: Graphical representation of variation of r_1 for x(t).

in the self-reproduction rate (r_1) of Tea plant. With the increase in the self-reproduction rate (r_1) , the tea plants x(t), pests that damage the tea plants y(t), and reasonable competitor for pests z(t) increases simultaneously. Effect of Intensity of competition (c_1) : Effect of the intensity of competition (c_1) among tea plants for food, space, etc., on x(t), y(t), z(t) seen in the Figures 11-13. With the increase in the intensity of competition (c_1) , the tea plants x(t), pests that damage the tea plants y(t), and reasonable competitor for pests z(t) decreases simultaneously.

6. Conclusion

In this article, we have considered a novel method called the Haar wavelet collocation method (HWCM) to study the nonlinear model of control of biological pests in tea plants. Using the properties of the Haar wavelet and its operational matrix, the mathematical model has been transformed into a system of nonlinear algebraic equations. Newton's Raphson method was used to solve this system. The obtained numerical solution of tea model (1.1) was tabulated in tables. The absolute error of the HWCM has been tabulated by comparing the results obtained with the ND Solver solution. The obtained tables and graphs revealed that the HWCM converges rapidly. The obtained numerical results are represented in Tables 1-3 and Figures 2-4. As the resolution value (J) increases, the absolute error decreases and tends to zero. Figures 5-7 represent the graphical representation of the absolute error of HWCM (J=6,8,10) with ND Solver solution of x(t), y(t), and z(t). Figures 8-13 reveal the effect of self-reproduction rate (r_1) and intensity of competition (c_1) on tea plants x(t), pests that damage the tea plants y(t), and reasonable competitor for pests z(t). Hence, the results show that the HWCM can solve the problem more precisely. This method can be applied to other biological models of different order with slight changes in the method. Also, the current approach is not restricted to a system of ODEs. It can be extended to partial differential equations and, more broadly, to fractional ones.

Acknowledgment: The author expresses his affectionate thanks to the DST-SERB, Govt. of India. New Delhi for the financial support under Empowerment and Equity Opportunities for Excellence in Science for 2023-2026. F.No.EEQ/2022/620 Dated:07/02/2023.

Declarations

Ethical Approval: Not applicable.

Funding: The author states that no funding is involved.

Availability of data and materials: The data supporting this study's findings are available within the article.

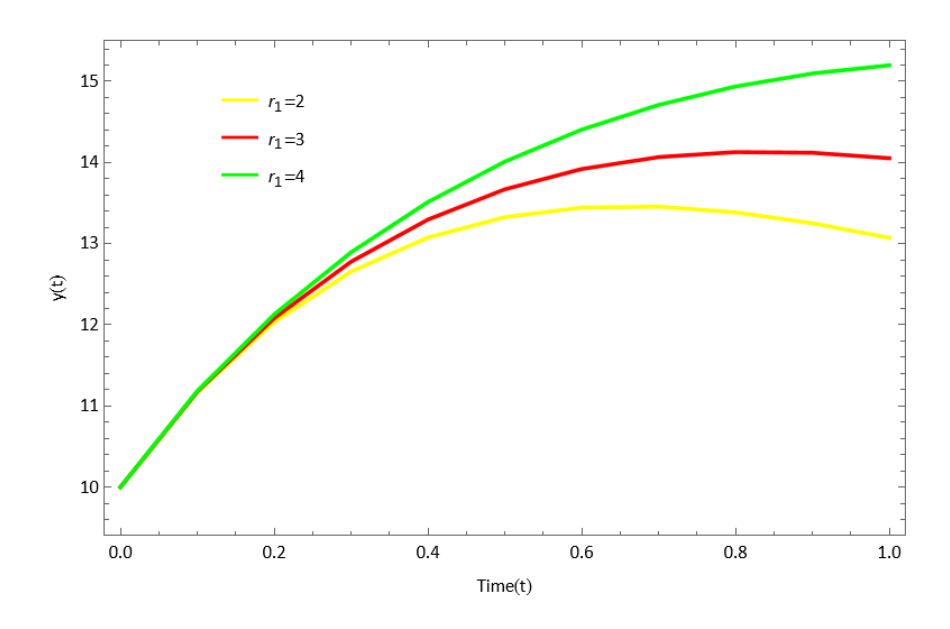


Figure 9: Graphical representation of variation of r_1 for y(t).

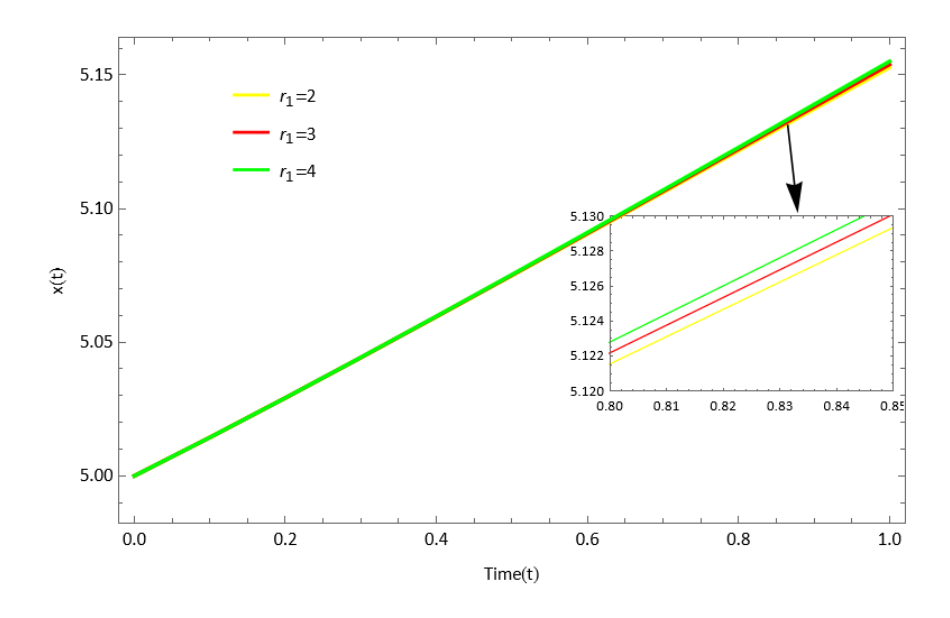


Figure 10: Graphical representation of variation of r_1 for z(t).

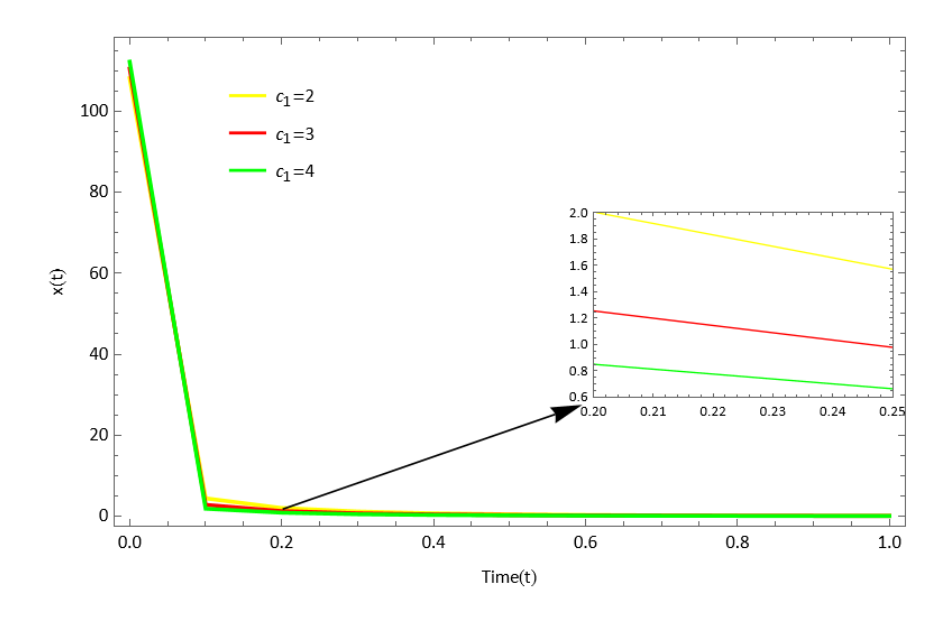


Figure 11: Graphical representation of variation of c_1 for $\boldsymbol{x}(t).$

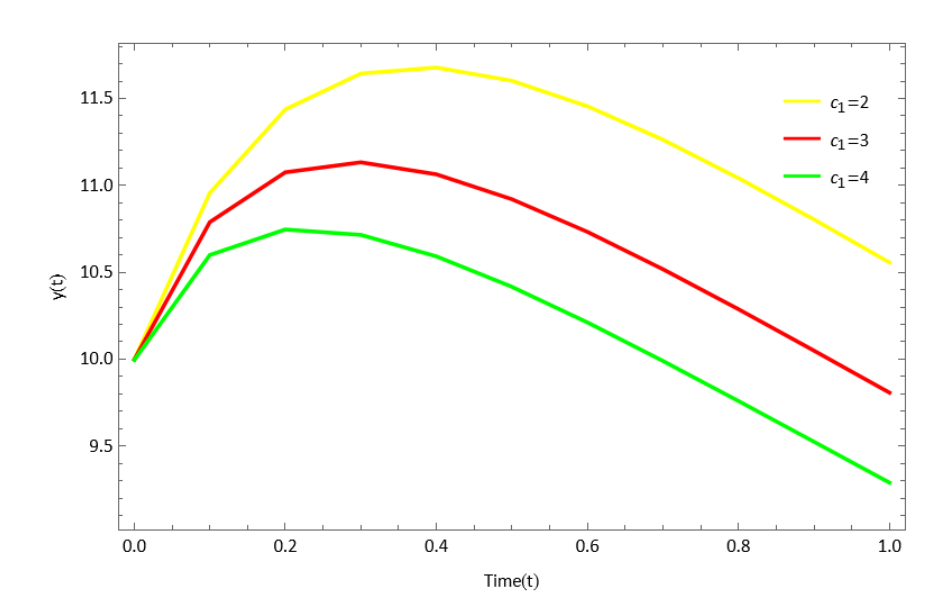


Figure 12: Graphical representation of variation of c_1 for y(t).

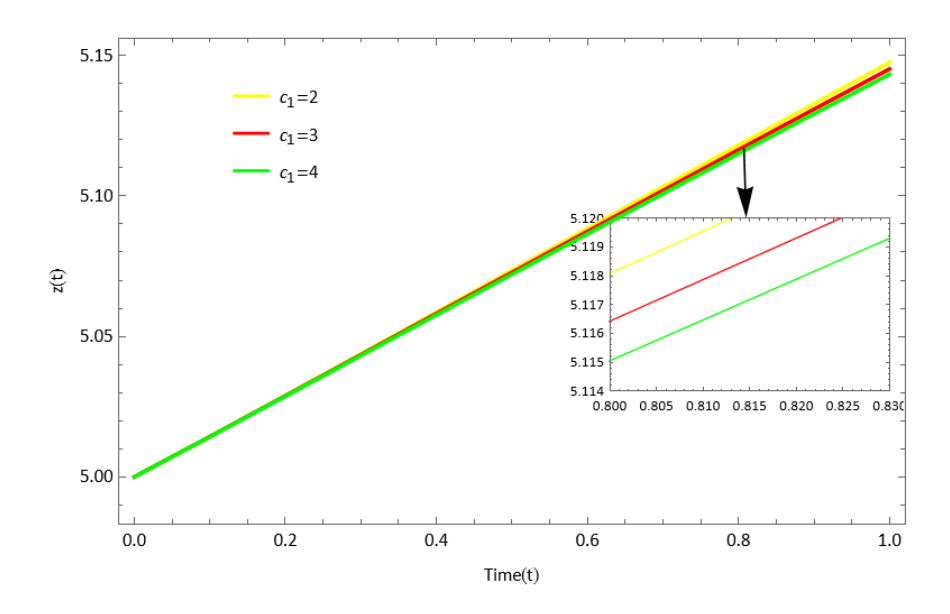


Figure 13: Graphical representation of variation of c_1 for z(t).

References

- [1] Basu Majumder, A., Bera, B., and Rajan, A. (2010). Tea statistics: global scenario. Inc J Tea Sci, 8(1), 121-4.
- [2] Zafar, Z. U. A., Shah, Z., Ali, N., Alzahrani, E. O., and Shutaywi, M. (2021). Mathematical and stability analysis of fractional order model for spread of pests in tea plants. Fractals, 29(01), 2150008. https://doi.org/10.1142/S0218348X21500080
- [3] Hazarika, L. K., Bhuyan, M., and Hazarika, B. N. (2009). Insect pests of tea and their management. Annual review of entomology, 54, 267-284.
- [4] Maiti, A., Patra, B., and Samanta, G. P. (2006). Sterile insect release method as a control measure of insect pests: a mathematical model. Journal of Applied Mathematics and Computing, 22, 71-86.
- [5] Pathak, S., and Maiti, A. (2010). Microbial pest control: A mathematical model. Journal of Biological Systems, 18(02), 455-478. https://doi.org/10.1142/S0218339010003317
- [6] Mamun, M. S. A., Ahmed, M., and Paul, S. K. (2014). Integrated approaches in tea pest management for sustainable tea production. In Proceedings of the Workshop on Tea Production Technology Updated (Vol. 24, pp. 18-32). Dhaka: 24 December 2014, organized by Bangladesh Tea Research Institute, Srimangal, Moulvibazar and Krishi Gobeshona Foundation, BARC campus.
- [7] Liu, S. S., Rao, A., and Vinson, S. B. (2014). Biological Control in China: Past, present and future—An introduction to this special issue. Biol. Control, 68(1), 5.10.1016/j.biocontrol.2013.05.005
- [8] Aktar, M. W., Sengupta, D., and Chowdhury, A. (2009). Impact of pesticides use in agriculture: their benefits and hazards. Interdisciplinary toxicology, 2(1), 1.
- [9] Wahab, S. (2004). Tea pests and their management with bio-pesticides. International Journal of Tea Science, 3(01 and 02).
- [10] Nakai, M. (2009). Biological control of tortricidae in tea fields in Japan using insect viruses and parasitoids. Virologica Sinica, 24, 323-332. https://doi.org/10.1007/s12250-009-3057-9
- [11] Achar, S. J., Baishya, C., Veeresha, P., and Akinyemi, L. (2021). Dynamics of fractional model of biological pest control in tea plants with Beddington–DeAngelis functional response. Fractal and Fractional, 6(1), 1.
- [12] Hastings, A., and Powell, T. (1991). Chaos in a three-species food chain. Ecology, 72(3), 896-903.
- [13] Panja, P., Mondal, S. K., and Jana, D. K. (2017). Effects of toxicants on Phytoplankton-Zooplankton-Fish dynamics and harvesting. Chaos, Solitons and Fractals, 104, 389-399. https://doi.org/10.1016/j. chaos.2017.08.036

- [14] Panja, P. (2019). Stability and dynamics of a fractional-order three-species predator-prey model. Theory in Biosciences, 138, 251-259.
- [15] Lepik, Ü. (2005). Numerical solution of differential equations using Haar wavelets. Mathematics and computers in simulation, 68(2), 127-143.
- [16] Lepik, Ü. (2007, March). Application of the Haar wavelet transform to solving integral and differential equations. In Proceedings of the Estonian Academy of Sciences, Physics, Mathematics (Vol. 56, No. 1).
- [17] Abbas, S., Tyagi, S., Kumar, P., Ertürk, V. S., Momani, S. (2022). Stability and bifurcation analysis of a fractional-order model of cell-to-cell spread of HIV-1 with a discrete time delay. Mathematical Methods in the Applied Sciences, 45(11), 7081-7095.
- [18] Qureshi, S., Yusuf, A., Shaikh, A. A., Inc, M., Baleanu, D. (2019). Fractional modeling of blood ethanol concentration system with real data application. Chaos: An Interdisciplinary Journal of Nonlinear Science, 29(1). Math Comput Simul 1997;44(5):457–70.
- [19] Shiralasetti, S., and Kumbinarasaiah, S. (2017). Some results on Haar wavelets matrix through linear algebra. Wavelet and Linear Algebra, 4(2), 49-59.
- [20] Preetham, M. P., and Kumbinarasaiah, S. (2023). A numerical study of two-phase nanofluid MHD boundary layer flow with heat absorption or generation and chemical reaction over an exponentially stretching sheet by Haar wavelet method. Numerical Heat Transfer, Part B: Fundamentals, 1-30.
- [21] Darweesh, A., Al-Khaled, K., and Al-Yaqeen, O. A. Haar Wavelets Method for Solving Class of Coupled Systems of Linear Fractional Fredholm Integro-Differential Equations. Heliyon. 10.1016/j.heliyon. 2023.e19717
- [22] Kumbinarasaiah, S., and Manohara, G. (2023). Modified Bernoulli wavelets functional matrix approach for the HIV infection of CD4+ T cells model. Results in Control and Optimization, 10, 100197.
- [23] Shiralashetti, S. C., and Kumbinarasaiah, S. (2020). Laguerre wavelets exact parseval frame-based numerical method for the solution of system of differential equations. International Journal of Applied and Computational Mathematics, 6, 101, 1-16. https://doi.org/10.1007/s40819-020-00848-9
- [24] Vivek, Kumar, M., and Mishra, S. N. (2023). Solution of linear and nonlinear singular value problems using operational matrix of integration of Taylor wavelets. Journal of Taibah University for Science, 17(1), 2241716.
- [25] Srinivasa, K., Baskonus, H. M., and Guerrero Sánchez, Y. (2021). Numerical solutions of the mathematical models on the digestive system and covid-19 pandemic by hermite wavelet technique. Symmetry, 13(12), 2428.
- [26] Majak, J., Shvartsman, B. S., Kirs, M., Pohlak, M., Herranen, H. (2015). Convergence theorem for the Haar wavelet based discretization method. Composite Structures, 126, 227-232. https://doi.org/10.1016/j.compstruct.2015.02.050
- [27] Chen, C. F., Hsiao, C. H. (1997). Haar wavelet method for solving lumped and distributed-parameter systems. IEE Proceedings-Control Theory and Applications, 144(1), 87-94.
- [28]] Hsiao CH. State analysis of the linear time delayed systems via Haar wavelets. Math Comput Simul 1997;44(5):457–70.
- [29] Ramzan, M., Nazar, M. (2022). Thermo-diffusion effect on magnetohydrodynamics flow of fractional Casson fluid with heat generation and first order chemical reaction over a vertical plate. Journal of Mathematical Analysis and Modeling, 3(2), 8-35. doi:10.48185/jmam.v3i2.322
- [30] Asjad, M. I., Aleem, M., Ali, W., Abubakar, M., Jarad, F. (2021). Enhancement of heat and mass transfer of a physical model using Generalized Caputo fractional derivative of variable order and modified Laplace transform method. Journal of Mathematical Analysis and Modeling, 2(3), 41-61. doi:10.48185/jmam.v2i3.380
- [31] Shah, K., Amin, R., Abdeljawad, T. (2023). Utilization of Haar wavelet collocation technique for fractal-fractional order problem. Heliyon.
- [32] Reunsumrit, J., Shah, K., Khan, A., Amin, R., Ahmad, I., Sitthiwirattham, T. (2023). Extension Of Haar Wavelet Techniques For Mittag-Leffler Type Fractional Fredholm Integro-Differential Equations. Fractals, 31(02), 2340038.
- [33] Amin, R., Shah, K., Awais, M., Mahariq, I., Nisar, K. S., Sumelka, W. (2023). Existence And Solution Of Third-Order Integro-Differential Equations Via Haar Wavelet Method. Fractals, 31(02), 2340037.
- [34] Amin, R., Shah, K., Gao, L., Abdeljawad, T. (2023). On existence and numerical solution of higher order nonlinear integro-differential equations involving variable coefficients. Results in Applied Mathematics, 20, 100399. https://doi.org/10.1016/j.rinam.2023.100399